

1 **Technical Note: Monte-Carlo genetic algorithm (MCGA) for**  
2 **model analysis of multiphase chemical kinetics to determine**  
3 **transport and reaction rate coefficients using multiple**  
4 **experimental data sets**

5  
6 **Thomas Berkemeier<sup>1,2</sup>, Markus Ammann<sup>3</sup>, Ulrich K. Krieger<sup>4</sup>, Thomas Peter<sup>4</sup>, Peter**  
7 **Spichtinger<sup>5</sup>, Ulrich Pöschl<sup>1</sup>, Manabu Shiraiwa<sup>1,6</sup> and Andrew J. Huisman<sup>7</sup>**

8 [1] Max Planck Institute for Chemistry, Multiphase Chemistry Department, 55128, Mainz,  
9 Germany

10 [2] Georgia Institute of Technology, School of Chemical and Biomolecular Engineering, 30320,  
11 Atlanta, GA, USA

12 [3] Paul Scherrer Institute, Laboratory of Environmental Chemistry, 5232, Villigen, Switzerland

13 [4] ETH Zurich, Institute for Atmospheric and Climate Science, 8092, Zurich, Switzerland

14 [5] Johannes Gutenberg University, Institute for Atmospheric Physics, 55128, Mainz, Germany

15 [6] University of California, Irvine, Department of Chemistry, 92697, Irvine, CA, USA

16 [7] Union College, Department of Chemistry, 12308, Schenectady, NY USA

17

18 Corresponding Authors: T. Berkemeier ([thomas.berkemeier@chbe.gatech.edu](mailto:thomas.berkemeier@chbe.gatech.edu)) and A. J.

19 Huisman ([huismana@union.edu](mailto:huismana@union.edu))

## 20 **Abstract**

21 We present a Monte-Carlo Genetic Algorithm (MCGA) for efficient, automated and unbiased  
22 global optimization of model input parameters by simultaneous fitting to multiple experimental  
23 data sets. The algorithm was developed to address the inverse modelling problems associated with  
24 fitting large sets of model input parameters encountered in state-of-the-art kinetic models for  
25 heterogeneous and multiphase atmospheric chemistry. The MCGA approach utilizes a sequence  
26 of optimization methods to find and characterize the solution of an optimization problem. It  
27 addresses an issue inherent to complex models whose extensive input parameter sets may not be  
28 uniquely determined from limited input data. Such ambiguity in the derived parameter values can  
29 be reliably detected using this new set of tools, allowing users to design experiments that should  
30 be particularly useful to constrain model parameters. We show that the MCGA algorithm has been  
31 used successfully to constrain parameters such as chemical reaction rate coefficients, diffusion  
32 coefficients and Henry's law solubility coefficients in kinetic models of gas uptake and chemical  
33 transformation of aerosol particles as well as multiphase chemistry at the atmosphere-biosphere  
34 interface. While this study focuses on the processes outlined above, the MCGA approach should  
35 be portable to any numerical process model with similar computational expense and extent of the  
36 fitting parameter space.

37

38

## 39 1. Introduction

40 Atmospheric aerosols play a key role in climate, air quality and public health. Heterogeneous  
41 reactions and multiphase processes alter the physical and chemical properties of organic aerosol  
42 particles, but the effects of these reactions are not fully elucidated (e.g. Finlayson-Pitts,  
43 2009;George and Abbatt, 2010;Abbatt et al., 2012;Pöschl and Shiraiwa, 2015). While multiphase  
44 chemistry in aerosols and clouds can be described by a sequence of well-understood physical and  
45 chemical elementary processes in kinetic models (Hanson et al., 1994;Pöschl et al., 2007;George  
46 and Abbatt, 2010), the deduction of parameters or rate coefficients of the individual elementary  
47 processes is severely complicated by the inherent coupling of chemical reactions and mass  
48 transport processes (Kolb et al., 2010;Berkemeier et al., 2013;Shiraiwa et al., 2014).

49 Heterogeneous chemical reactions on aerosol particles are traditionally described using so-called  
50 "resistor" models, which represent parallel and sequential physical or chemical processes in  
51 analogy to electrical circuits. These models have typically been used to derive analytical  
52 expressions for simplified limiting cases (e.g. Hanson et al., 1994;Worsnop et al., 2002;Hearn et  
53 al., 2005). Recently, numerical models have been developed that allow a more complete  
54 consideration of the time- and depth-resolved chemical and physical behaviour of aerosol particles,  
55 leading to a better understanding of these reaction systems, especially under conditions where the  
56 steady-state assumptions underlying the resistor models are not valid (Smith et al., 2003;Pöschl et  
57 al., 2007;Steimer et al., 2015;Berkemeier et al., 2016). Kinetic multi-layer models describe single  
58 particles or thin films by division into compartments such as near-surface gas phase, surface and  
59 particle bulk, and further subdivision of the particle bulk into thin layers to achieve depth-  
60 resolution. Specific models provide a focus on chemistry such as KM-SUB (Shiraiwa et al., 2010),  
61 on gas-particle partitioning such as KM-GAP (Shiraiwa et al., 2012) and ADCHAM (Roldin et al.,

62 2014), or on water diffusion such as the ETH Diffusion Model (Zobrist et al., 2011). For simplicity,  
63 throughout this manuscript we refer to a “kinetic model” as any computational model that is used  
64 to simulate a system’s behaviour. We will use the term “input parameters” to address the prescribed  
65 model parameters (thermodynamic, kinetic, or physical) that are optimized in this study so that  
66 kinetic model output matches experimental data, a process that we will refer to as “fitting the  
67 kinetic model”. Note that this definition excludes model parameters that are clearly defined by  
68 physical laws or the experiment (e.g. physical constants, experimental conditions) or are of purely  
69 technical nature (e.g. integration time steps).

70 Ideally, fitting a kinetic model to experimental data would return all chemical and physical  
71 parameters necessary to understand the importance of the processes at work and to predict the  
72 outcome of future experiments, even if conducted under experimental conditions not part of the  
73 training data set, i.e. all experimental data used during the fitting process. However, kinetic models  
74 often require a multitude of input parameters, some of which are not constrained well  
75 experimentally or are merely effective parameters combining a sequence of inherently coupled  
76 processes. In general, two main difficulties arise when optimizing complex models to experimental  
77 data:

78 (1) The optimization hyper surface is often non-convex, i.e., it will not have only a single minimum  
79 due to interactions between non-orthogonal (coupled) input parameters and/or scatter in the  
80 experimental data. Hence, steepest descent methods fail since they get trapped easily in local  
81 minima. Brute-force or exhaustive searches, where an  $n$ -dimensional grid is applied to the input  
82 parameter space and the fit quality evaluated for every grid point in all  $n$  dimensions, are often not  
83 computationally feasible.

84 (2) If too little or too similar experimental data is used during the fitting process or input  
85 parameters are allowed to move in a large range, the optimization problem can be underdetermined  
86 (ill-defined) and multiple solutions may exist. In this case, even though a good agreement between  
87 model output and training data set is obtained, it is likely that only the model input parameters  
88 corresponding to the most limiting processes will be physically meaningful. Extrapolation of the  
89 model outside its training range can then lead to strong discrepancies between modelled and  
90 measured data. For example, if a model is trained using data that is exclusively limited by a single  
91 process, it will constrain the parameters that represent that specific process while the other  
92 parameters remain nearly unconstrained even if multiple data sets are used. This means that a  
93 parameter set were optimized using data from surface film experiments, the bulk diffusion  
94 coefficients would likely be poorly constrained regardless of how many different experimental  
95 datasets of that type were used.

96 Hence, sophisticated optimization methods are needed, which quickly and reliably determine the  
97 model input parameters that lead to the best correlation between kinetic model and experiment.  
98 Furthermore, experiments covering a broad range of conditions must be conducted to ensure that  
99 the observables are controlled by (a) as many model input parameters as possible across all  
100 experimental conditions, but (b) by as few model input parameters as possible for a specific  
101 experimental condition (i.e. limiting cases). The MCGA algorithm presented here is able to  
102 overcome the difficulty of a complex optimization hypersurface with many local minima while  
103 providing the user with a realistic assessment of how well-constrained the model input parameters  
104 are by the experimental data.

105

## 106 **2. Monte-Carlo Genetic Algorithm (MCGA)**

107 In many modelling applications, methods are needed that reliably find the optimum in non-convex  
108 optimization problems and detect underdetermined optimization problems. Global optimization  
109 methods have been subject of extensive research in the past (Arora et al., 1995) and provide means  
110 of approximating non-convex optimization problems without premature convergence to local  
111 optima. Examples for these methods are simulated annealing methods and evolutionary  
112 algorithms. In atmospheric chemistry, simple optimization techniques are commonly used to  
113 determine kinetic parameters by fitting of rate equations to experimental data sets, but to our  
114 knowledge no global optimization technique diligently designed for the determination of  
115 atmospheric reaction rate coefficients from multiple data sets was described thus far. A related  
116 technique (Monte-Carlo Markov Chain algorithm) has been used to determine parametric  
117 uncertainties in cloud-aerosol interaction models (Partridge et al., 2012;Lowe et al., 2016). Global  
118 optimization was also used to calculate thermodynamic equilibria for phase separation of aqueous  
119 multicomponent solutions (Zuend and Seinfeld, 2013).

120 In this study, we present the Monte-Carlo Genetic Algorithm (MCGA), a method combining direct  
121 Monte-Carlo sampling with a genetic algorithm as a heuristic global optimization method that  
122 approximates the global optimum for input parameter sets of computational models. Repeated  
123 execution of the search algorithm can be used to test for uniqueness or to provide statistical bounds  
124 on the model input parameters. The MCGA algorithm utilizes a two-step approach to find minima  
125 on non-convex hyper surfaces. First, a Monte-Carlo (MC) sampling is performed in the large space  
126 of possible model input parameters to narrow down the possible solution to smaller areas of  
127 interest. The parameter sets are evaluated using a goodness-of-fit expression of the user's choice,  
128 such as the root-mean-square (RMS) error between kinetic model output and experimental data.

129 In the examples presented here, the RMS error or logarithmic RMS error was used. When multiple  
130 datasets were fitted, a weighting factor was introduced to prevent bias due to the number of data  
131 points in different experimental datasets. An additional optional weighting factor allows the user  
132 to assign priority to experimental data with lower statistical error or scatter. The parameter sets for  
133 the MC sampling are generated randomly from a distribution of the model input parameters. Each  
134 parameter was sampled using a logarithmically spaced distribution of values to provide uniform  
135 sampling over the large ranges most input parameters can possibly adopt. Note that, depending on  
136 the problem, different distributions and sampling strategies (e.g. Latin hypercube sampling) could  
137 be applied.

138 The genetic algorithm (GA) uses survival of the fittest to optimize an ensemble (the *population*)  
139 of parameter sets (the *individuals*) over several iterations (the *generations*). Processes known from  
140 natural evolution such as survival, recombination, mutation and migration are mimicked to  
141 optimize a population. The initial population is formed by the parameter sets with the best  
142 goodness-of-fit obtained in the MC sampling step. An equal number of random parameter sets are  
143 added to ensure diversity within the pool of parameter sets and counteract sampling bias from  
144 shallow local minima (Fig. 1).

145 During execution of the GA, a number of model input parameter sets with the highest correlation  
146 between model output and experimental data (goodness-of-fit) are directly transferred into the next  
147 generation by the survival mechanism (the *elites*). The remaining population is generated using  
148 combinations of parameters from the individuals in the previous generation with moderate or better  
149 goodness-of-fit (the *parents*), forming the *children* for the next generation. In this study, 5% of the  
150 next generation are elite individuals, which are transferred with no changes, while 80 % of the  
151 children is created by randomly choosing individual parameters (*genes*) from two selected parents

152 with equal weighting. The higher the goodness-of-fit of a certain individual, the higher is its  
153 likeliness to be selected as parent. This way, parameters leading to high goodness-of-fit are  
154 positively reinforced, leading to improvement and slow homogenization of the population. Finally,  
155 20 % of children are created by applying a mutation scheme that alters parameters in a stochastic  
156 manner within the prescribed bounds to enhance genetic variability. Collectively, these  
157 mechanisms enable the MCGA to overcome local minima, a crucial feature of a global  
158 optimization method. Iteration of these steps eventually results in a homogeneous, optimized  
159 population and the common parameter set is taken as result. The MCGA can be run multiple times  
160 to generate a set of representative solutions, which has been the default approach in previous  
161 applications of MCGA (cf. Sect. 4). With only few (~5-10) repetitions, this procedure allows the  
162 user to assure full convergence to the global optimum. In addition, the random sampling of  
163 optimization space between different executions of MCGA will generate statistical bounds on the  
164 parameters if a sufficiently large number of repetitions is computationally feasible.

165 In this study we used the genetic algorithm provided by MathWorks<sup>®</sup> (Matlab<sup>®</sup> Global  
166 Optimization Toolbox) and developed a routine for parallel computation on computer clusters. In  
167 a typical setting, the MC step and GA step of the optimization occupied an approximately equal  
168 amount of computation time. Figure 2 describes the implementation of the parallel MCGA  
169 optimization method. The  $N$  parallel threads share common populations of parameter sets that are  
170 iteratively optimized by extracting a subset of parameter sets and performing the genetic algorithm  
171 on this subset. Once a sub-evaluation of the genetic algorithm has finished, the parameter sets are  
172 mixed into the population, and after randomization, a different subset of parameter sets is extracted  
173 and their optimization is immediately continued. Since the parallel threads will run



174 asynchronously, a fraction of individuals must remain in the population to be mixed with, to enable  
175 continuous operation without waiting times.

176

### 177 **3. Implications for modelling and measuring chemical kinetics**

178 Although models may possess a multitude of kinetic and thermodynamic input parameters that  
179 represent the many possible sequential and/or concurrent processes occurring in the system, their  
180 behaviour is often driven by only a single or at most a few processes at a certain point in time. In  
181 chemical kinetics, the behaviour of the system can often be characterized by a kinetic regime,  
182 which may change during the course of the reaction and with experimental conditions (Berkemeier  
183 et al., 2013). If a set of model input parameters can be uniquely determined (by MCGA or another  
184 means) and results in a high-fidelity fit of model output to experimental data, the parameters then  
185 would be regarded as correct within the approximations of the underlying model and uncertainties  
186 of the experimental data. This is a convenient way to assimilate data from multiple previous  
187 studies; data sets can be weighted to reflect confidence in their results, and the final range of  
188 accepted parameters then represents a consensus from the fitted data. However, it may not always  
189 be possible to fully constrain the input parameters, even using multiple experimental datasets. In  
190 general, there are two reasons that a model input parameter can remain unconstrained after  
191 optimization:

- 192 (i) the parameter is non-influential, or
- 193 (ii) the parameter is inherently coupled to another one, forming a non-orthogonal parameter  
194 pair under all experimental conditions.

195 Fig. 3 illustrates both cases in an example taken from atmospheric multiphase chemistry, using the  
196 benchmark system of ozone + oleic acid and data adopted from Hearn *et al.* (2005). The original  
197 data was converted from ozone exposure to a time series using an ozone concentration of  $2.76 \times 10^{15}$   
198  $\text{cm}^{-3}$ . The MCGA algorithm was executed under a constrained parameter set, in which only  
199 desorption lifetime and surface reaction rate coefficient were allowed to vary. In this scenario,  
200 repeated execution of MCGA returned multiple solutions, for which the model output had nearly  
201 equivalent goodness-of-fit with only slight variance between them (Fig. 3A). In stark contrast to  
202 the uniform correlation between model output and experimental data, Fig. 3B shows the high  
203 variance within the model parameters yielding these solutions (red markers) which scatter across  
204 a narrow valley of the optimization hypersurface (contour lines). In the upper portion of the figure,  
205 i.e. above a desorption lifetime of  $10^{-4}$  s, a vertical relationship between both parameters indicates  
206 that the desorption lifetime is a non-influential parameter and can take on any value in this interval,  
207 corresponding to case (i) above. In the lower portion of the figure, i.e. below a desorption lifetime  
208 of the diagonal relationship indicates that an increase in one parameter can be compensated with a  
209 decrease in the other parameter and both form a non-orthogonal pair, corresponding to case (ii)  
210 above. For comparison, Figs. 3C and 3D show examples of optimization hypersurfaces from  
211 Berkemeier *et al.* (2016), who studied multiphase ozonolysis of shikimic acid and investigated the  
212 existence of non-orthogonal parameter pairs by varying optimized parameters ( $\lambda_i$ ) by a factor  $f(\lambda_i)$   
213 to depict the total residual as a 2D contour map. Fig. 3C shows that the Henry's law coefficient  
214 for ozone ( $H_{\text{cp},\text{O}_3}$ ) and the product of the bulk reaction rate coefficient ( $k_{\text{BR}}$ ) with the bulk  
215 diffusivity of ozone ( $D_{\text{b},\text{O}_3}$ ) and the bulk-to-surface transport coefficient of ozone ( $k_{\text{bs},\text{O}_3}$ ) are fully  
216 non-orthogonal. Figure 3D shows a single, well-defined optimum parameter set for the effective

217 molecular cross section of ozone ( $\sigma_{O_3}$ ) and the desorption lifetime of ozone ( $\tau_{d,O_3}$ ), indicating that  
218 these parameters are fully orthogonal for the experimental data fit in that study.

219 The prerequisite of a successful optimization is to fit a sufficiently broad experimental data set so  
220 that a unique and accurate set of fitting parameters is obtained. Thus, both of the above conditions  
221 must be avoided. This may be achieved by including additional experimental data, especially from  
222 a different experimental technique or over a different timescale so that the system might sample  
223 another limiting behaviour. In the data given in Fig. 3 above, for example, measuring full time  
224 series at different oxidant concentrations may help to constrain the oxidant's desorption lifetime.  
225 However, if a model has too many free parameters (or especially parameters that are not well-  
226 constrained by experimental data), it may be necessary to reduce the model complexity or fix some  
227 of the parameters. We therefore recommend using data sets obtained from a range of different  
228 experimental techniques to ensure this variability if they are available, and using models with as  
229 few free parameters as possible.

230 In the example above, it was possible to use brute-force sampling to determine the true  
231 optimization hypersurface (contour lines) for comparison to the MCGA results. Of course, in  
232 typical applications, the number and range of input parameters makes such a search prohibitive.  
233 The computational feasibility of an optimization depends crucially on the size of the input  
234 parameter space, i.e. number and possible range of all parameters. Using an unreasonably large  
235 range for input parameters increases the possibility of finding non-physical solutions that fit the  
236 experimental data. The input parameter space can be reduced based on *a priori* knowledge from  
237 laboratory experiments and theoretical calculations. Parameters can be narrowed down by  
238 laboratory experiments (e.g. bulk experiments for derivation of trace gas solubility), by physics  
239 (e.g. the upper limit of the accommodation coefficient at unity), or by simulations (e.g., molecular

240 dynamics simulations to estimate the surface accommodation coefficient and desorption lifetime  
241 as in Vieceli et al. (2005) and Julin et al. (2013)). Note that in the example given in Fig. 3b, the  
242 two parameters were not truly independent, so that constraining either model parameter from *a*  
243 *priori* information would constrain the other parameter. In multi-parameter optimizations, where  
244 many such dependencies might exist, this can lead to a significant reduction in solution space.

245

#### 246 **4. Application of MCGA in atmospheric multiphase chemistry**

247 The MCGA algorithm has been applied previously to chemical reaction systems of atmospheric  
248 relevance (Table 1). The essential parameters we use to describe an atmospheric multiphase  
249 chemical kinetic system of reactive trace gases X and bulk material Y include chemical reaction  
250 rate coefficients at the surface ( $k_{SLR}$ ) and in the bulk ( $k_{BR}$ ) of aerosol particles; bulk diffusion  
251 coefficients of reactive trace gases ( $D_{b,X}$ ) and the bulk matrix ( $D_{b,Y}$ ); accommodation coefficients  
252 ( $\alpha_{s,X}$ ) and desorption lifetimes ( $\tau_{d,X}$ ) of trace gases to the particle surface to determine transient and  
253 equilibrium adsorption behavior; and equilibrium constants for the solubility of reactive trace  
254 gases ( $K_{sol,cc,X}$ ), typically expressed in terms of Henry's law coefficients ( $H_{cp,X}$ ) (Pöschl et al.,  
255 2007; Ammann and Pöschl, 2007; Shiraiwa et al., 2010; Berkemeier et al., 2013).

256 In its first application the MCGA algorithm was used to fit individual data sets of the decay of  
257 oleic acid upon ozonolysis (Berkemeier et al., 2013), highlighting the need of fitting to multiple  
258 experimental data sets to constrain kinetic parameters. This was done in further studies that  
259 investigated gas uptake to (semi-)solid organic material in coated-wall flow-tube reactors (Arangio  
260 et al., 2015; Berkemeier et al., 2016), ozone-induced protein oligomerization in bulk solutions  
261 (Kampf et al., 2015), viscosity change upon alkene ozonolysis as measured with fluorescence

262 microscopy (Hosny et al., 2016), the redox-cycling reactions in the human lung lining fluid (Lakey  
263 et al., 2016a) as well as ozonolysis of squalene contained in human skin lipids (Lakey et al.,  
264 2016b). In each of these studies, a large set of model input parameters was optimized to several  
265 experimental data sets to constrain the input parameter space. In the following, we review results  
266 previously obtained by the MCGA algorithm to demonstrate its utility in determining kinetic  
267 parameters, assimilating large datasets, and detecting ill-defined problems.

268 In Berkemeier et al. (2016), 11 parameters were varied simultaneously to fit the ozone uptake to  
269 shikimic acid films over many hours, under 12 distinct experimental conditions, and using a single  
270 set of kinetic parameters (Fig. 4). The model was found to accurately describe the humidity- and  
271 concentration-dependence of ozone uptake and a high correlation between model output and  
272 experimental data was achieved. During optimization, a subset of six parameters, including  
273 diffusivity coefficients and trace gas solubility, was allowed to increase or decrease monotonically  
274 over 6 steps in relative humidity, resulting in a total of 41 optimized parameter values. Despite this  
275 large number of optimization parameters, a well-constrained parameter set could be obtained due  
276 to the large depth in training data and by applying *a priori* information.

277 In another study investigating the oxidation of biomass burning tracers with hydroxyl radicals  
278 (Arangio et al., 2015), repeated execution of MCGA revealed a remaining uncertainty in the kinetic  
279 parameters obtained from optimization to the two experimental data sets (Fig. 5). While some  
280 parameters could be narrowly constrained (diffusion coefficient of the organic matrix,  $D_{\text{org}}$ ), others  
281 were subject to larger uncertainties (surface layer reaction rate constant  $k_{\text{SLR}}$ , desorption lifetime  
282  $\tau_d$ ). Note that while these parameters seem almost unconstrained in Fig. 5, this uncertainty is due  
283 to the presence of non-orthogonal parameter pairs. As detailed in Fig. 3 and in Arangio et al.  
284 (2015), only specific combinations of the non-orthogonal parameters will lead to agreement

285 between model and experiment. This knowledge can be used to constrain these parameters in  
286 further experiments.

## 287 **5. Conclusions**

288 The MCGA algorithm addresses the problem of extracting physical and chemical parameters from  
289 experimental data. The algorithm allows the user to assimilate multiple datasets and its random  
290 sampling approach reduces the bias which may arise in more user-directed optimization methods.  
291 Unlike simple gradient-based optimization methods, MCGA can thus be used as a statistical tool  
292 that not only detects unconstrained parameters, but also finds dependencies between unconstrained  
293 parameters. The results can be applied in process models and may serve to direct future  
294 experimental studies, e.g. to drive a reaction system into regimes in which the remaining  
295 unconstrained parameters have high sensitivity. MCGA could also be used to constrain chemical  
296 reaction systems in the post-analysis of field and laboratory studies: starting with a large set of  
297 model input parameters (i.e. chemical reactions, physical processes), data from various  
298 measurement campaigns could be combined, reconciled and in a further step used to reduce the  
299 number of model input parameters to the key processes necessary to describe all measurement  
300 data. MCGA may be a powerful and useful tool to constrain kinetic parameters and reaction rate  
301 coefficients in models that study the formation of secondary organic aerosol in reaction chambers  
302 (Chan et al., 2007; Shiraiwa et al., 2013; Cappa et al., 2013; Riedel et al., 2016). It could be suitable  
303 for fine-tuning of reaction rates in large reaction mechanisms of atmospheric chemistry, such as  
304 the Master Chemical Mechanism (MCM; Jenkin et al., 1997; Saunders et al., 2003), the Gas-  
305 Aerosol Model for Mechanism Analysis (GAMMA; McNeill et al., 2012) or the Chemical  
306 Aqueous Phase Radical Mechanism (CAPRAM; Herrmann et al., 1999). Multiple experimental  
307 data sets from a broad range of techniques could be used with the algorithm to narrow down

308 difficult-to-measure reaction rate coefficients, provide uncertainty estimates and reconcile  
309 experiments across different research groups and facilities.

### 310 **Acknowledgements**

311 T. Berkemeier was supported by the Max Planck Graduate Center with the Johannes Gutenberg-  
312 Universität Mainz (MPGC). A. J. Huisman was supported by the United States National Science  
313 Foundation under award no. IRFP 1006117 and by ETH Zürich. Any opinions, findings, and  
314 conclusions or recommendations expressed in this material are those of the authors and do not  
315 necessarily reflect the views of the US National Science Foundation. We gratefully acknowledge  
316 G. D. Smith for providing published data in tabulated form. The authors like to thank A. Pozzer,  
317 C. Pfrang and C. Marcolli for stimulating discussions and support and J. Rieffel for his expertise  
318 in algorithms.

319 **Table 1.** Previous studies applying the MCGA algorithm.

<b>Study</b>	<b>Reaction system</b>
Berkemeier et al. (2013)	oleic acid + O <sub>3</sub>
Arangio et al. (2015)	levoglucosan and abietic acid + OH
Kampf et al. (2015)	protein + O <sub>3</sub>
Hosny et al. (2016)	oleic acid + O <sub>3</sub>
Berkemeier et al. (2016)	shikimic acid + O <sub>3</sub>
Tong et al. (2016)	OH formation by SOA decomposition in water
Lakey et al. (2016a)	reactive oxygen species and PM2.5 in lung lining fluid
Lakey et al. (2016b)	skin lipid (squalene) + O <sub>3</sub>

320



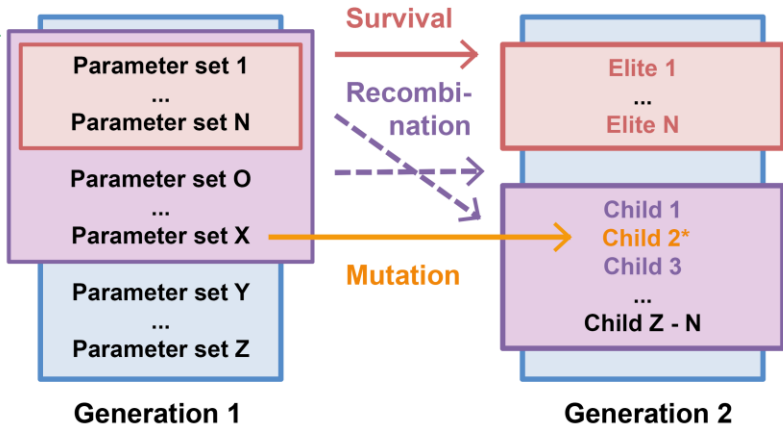
## Monte-Carlo sampling

Randomly sampled parameter sets

best  
random

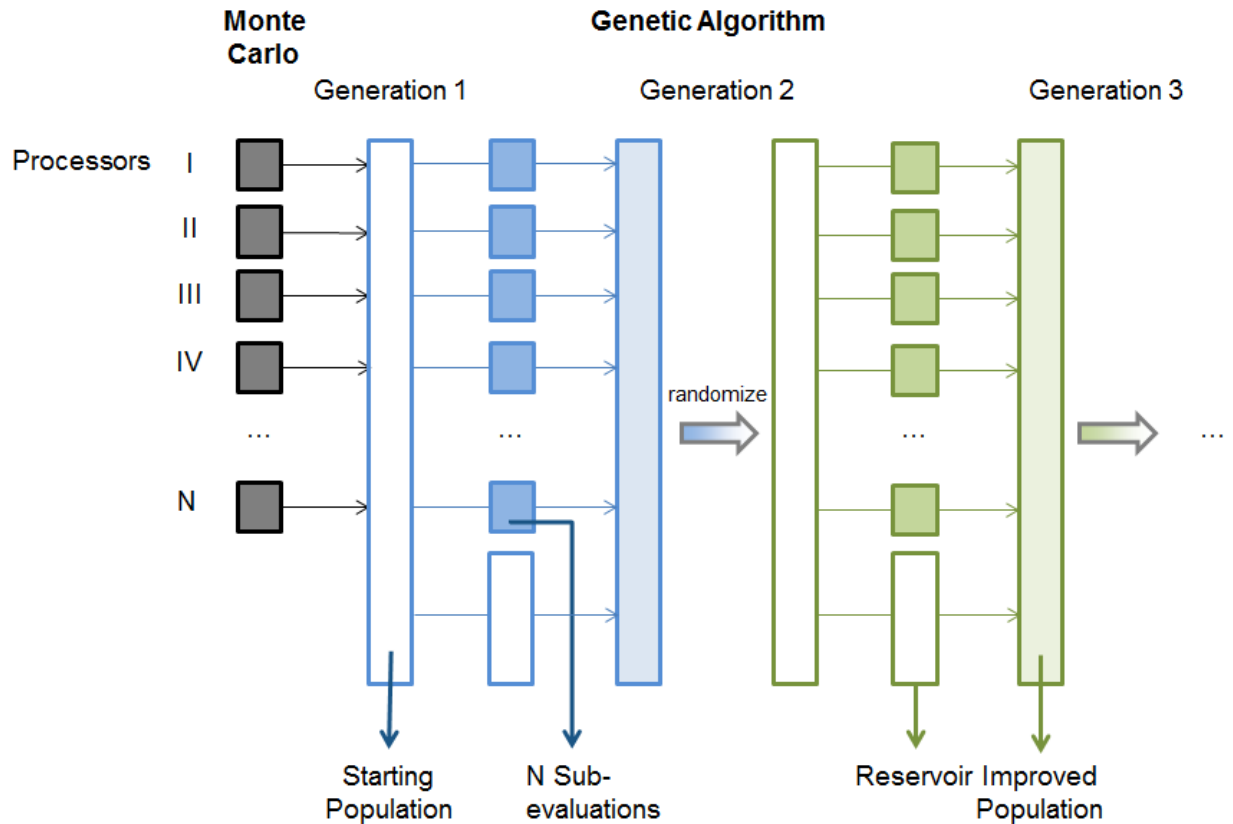
↑  
Goodness of fit

## Genetic Algorithm



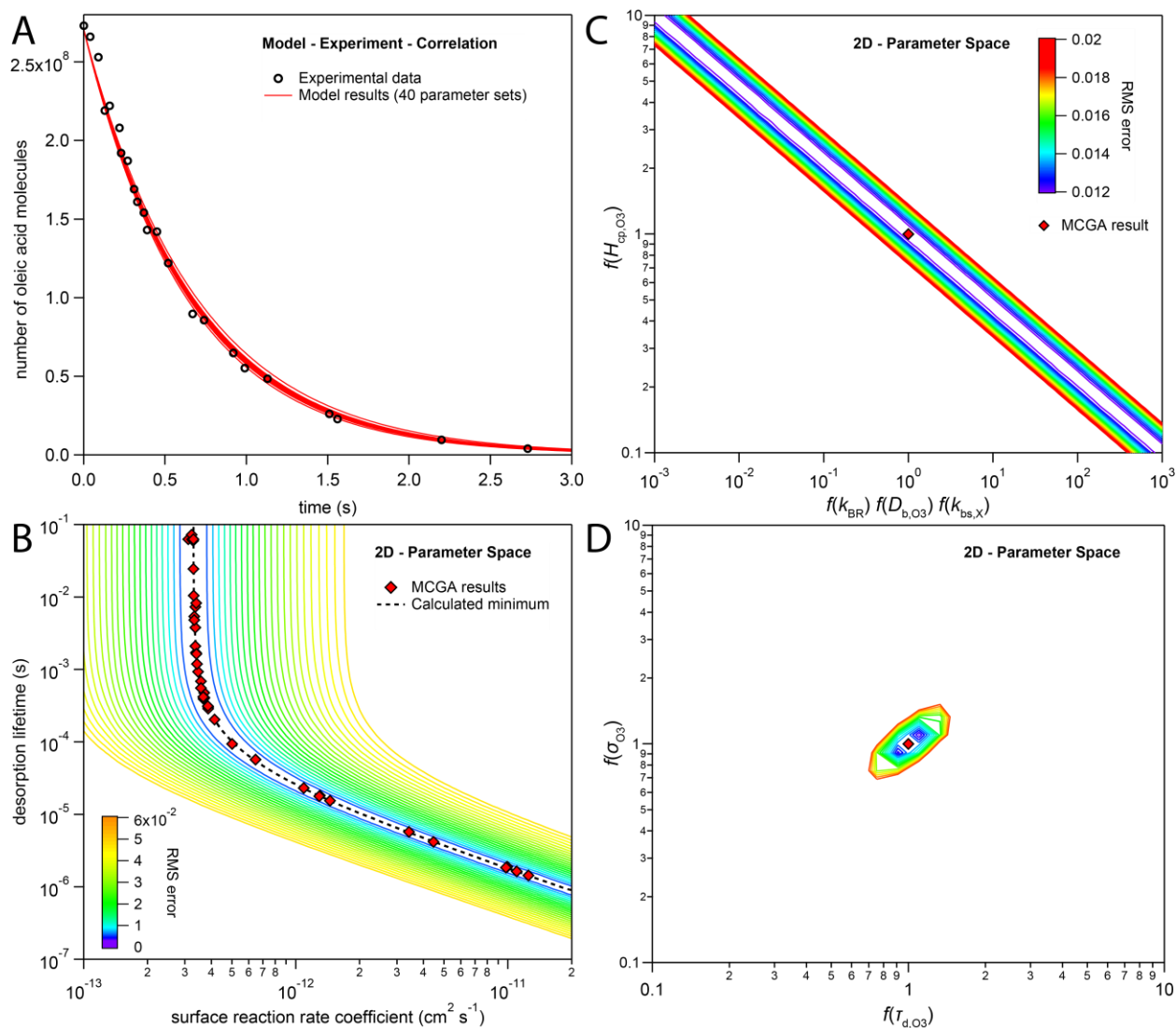
321

322 **Figure 1.** Schematic representation of the MCGA optimization method consisting of a Monte-Carlo  
323 sampling, which feeds into a genetic algorithm. *Populations* of model input parameter sets (blue boxes) are  
324 iteratively improved over several generations through survival of *elites* (red boxes) and recombination and  
325 mutation of *parents* to create *children* (purple boxes), until a sufficient correlation to the experimental data  
326 (goodness of fit) is obtained.



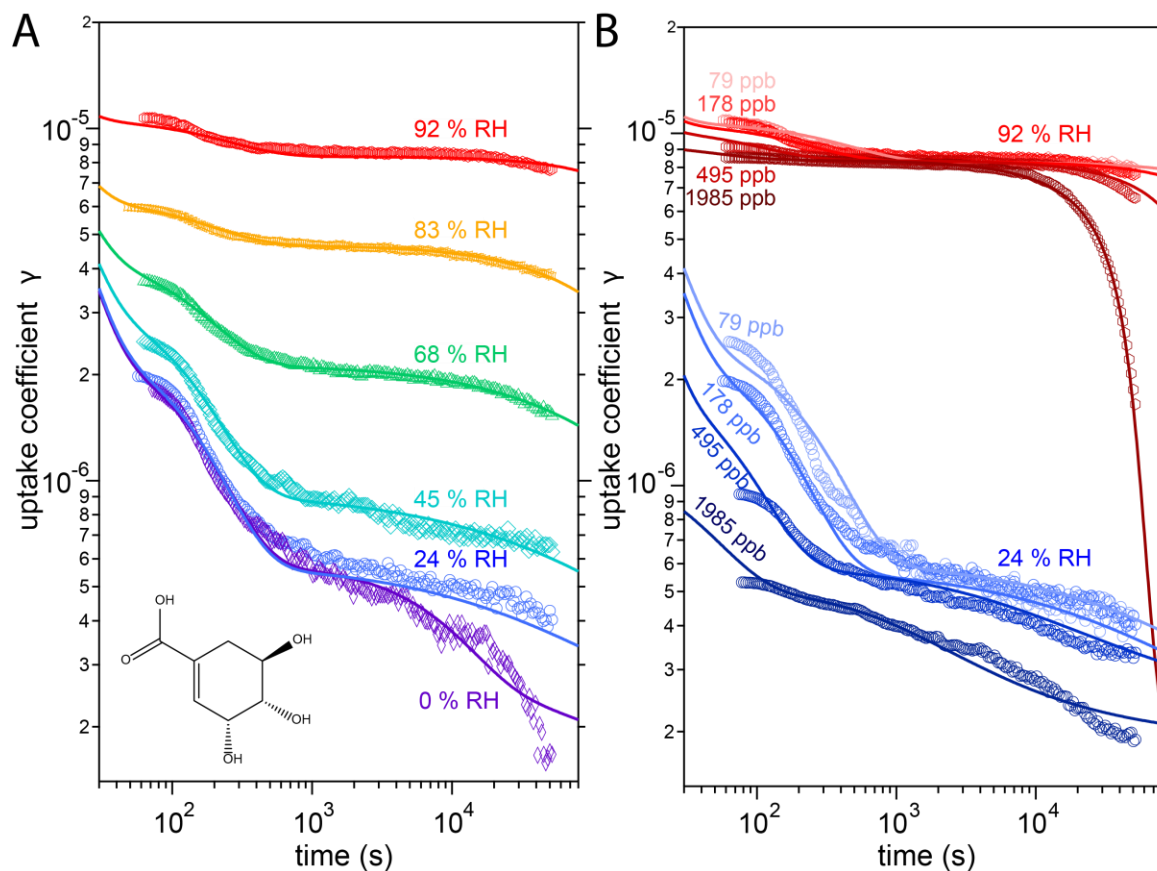
327

328 **Figure 2.** Schematic visualization of the parallelized MCGA optimization method. The Monte Carlo step  
 329 is performed independently on  $N$  processors and the best fitting parameter sets are fed along with random  
 330 parameter sets into the starting population. During the genetic algorithm step, each processor extracts a  
 331 number of parameter sets from the collective pool and performs a sub-evaluation of the genetic algorithm  
 332 on these parameter sets. After completion, the optimized parameter sets are fed back into the pool, which  
 333 always contains a non-zero number of parameter sets as reservoir. After randomization, a different  
 334 combination of parameter sets is extracted and the process repeated.

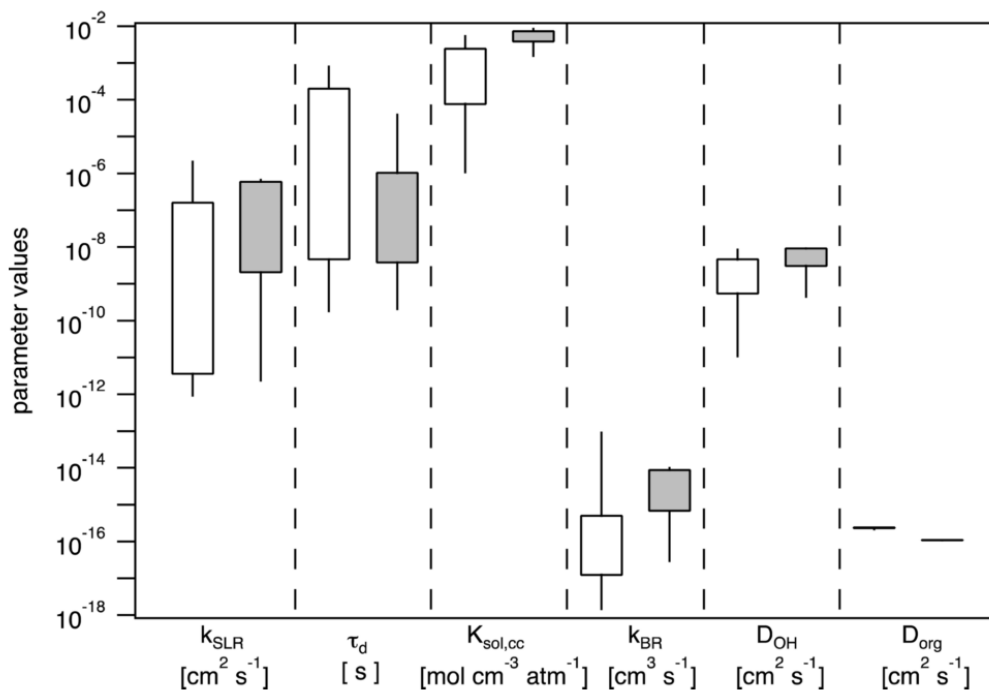


335  
 336 **Figure 3.** (A) Results from repeatedly fitting a kinetic model to a single experimental decay curve (adopted  
 337 from Hearn et al., 2005). MCGA was used to optimize two model parameters, a surface reaction rate  
 338 coefficient and the desorption lifetime of the gas phase oxidant. All other model parameters remained fixed.  
 339 (B) Visualization of MCGA algorithm's findings on the 2-dimensional optimization hypersurface. The  
 340 hypersurface (contour lines represent the root mean square deviances) exhibits no unique minimum due to  
 341 insufficiently broad experimental data and optimization results (red diamonds) scatter along the extended  
 342 minimum (black dashed line). (C) and (D) show exemplary optimization hypersurfaces with two parameters

343 showing an elongated (C) or a distinct minimum (D). Panels C and D are reproduced from Berkemeier et  
344 al. (2016) with permission from the PCCP Owner Societies.



345  
346 **Figure 4.** Observed (markers) and modelled (lines) uptake coefficients of ozone onto a thin film of shikimic  
347 acid as a function of exposure time. (A) Uptake coefficients at 178 ppb ozone gas phase concentration  $[O_3]_g$   
348 at different relative humidities of 0, 24, 45, 68, 83, and 92%. The structural formula of shikimic acid is  
349 displayed in the left bottom corner. (B) Uptake coefficients at 24% RH (blue solid lines) and 92% RH (red  
350 solid lines) with different  $[O_3]_g$  of 79, 178, 495, and 1985 ppb. Reproduced from Berkemeier et al. (2016)  
351 with permission from the PCCP Owner Societies.



352

353 **Figure 5.** Kinetic parameters for multiphase chemical reactions of OH with levoglucosan (white) and  
 354 abietic acid (gray) determined by the MCGA method of fitting the experimental data with the KM-GAP  
 355 model. The ranges of parameters are depicted as a box–whisker plot (the percentiles of 10, 25, 75, and 90%  
 356 are shown). Reprinted with permission from Arangio et al. (2015). Copyright 2015 American Chemical  
 357 Society.

## 358 References

- 359 Abbatt, J. P. D., Lee, A. K. Y., and Thornton, J. A.: Quantifying trace gas uptake to tropospheric  
360 aerosol: recent advances and remaining challenges, *Chem. Soc. Rev.*, 41, 6555-6581, 2012.
- 361 Ammann, M., and Pöschl, U.: Kinetic model framework for aerosol and cloud surface chemistry  
362 and gas-particle interactions - Part 2: Exemplary practical applications and numerical simulations,  
363 *Atmos. Chem. Phys.*, 7, 6025-6045, 2007.
- 364 Arangio, A. M., Slade, J. H., Berkemeier, T., Pöschl, U., Knopf, D. A., and Shiraiwa, M.:  
365 Multiphase Chemical Kinetics of OH Radical Uptake by Molecular Organic Markers of Biomass  
366 Burning Aerosols: Humidity and Temperature Dependence, Surface Reaction, and Bulk Diffusion,  
367 *J. Phys. Chem. A*, 119, 4533–4544, 10.1021/jp510489z, 2015.
- 368 Arora, J. S., Elwakeil, O. A., Chahande, A. I., and Hsieh, C. C.: Global optimization methods for  
369 engineering applications: A review, *Structural optimization*, 9, 137-159, 10.1007/bf01743964,  
370 1995.
- 371 Berkemeier, T., Huisman, A. J., Ammann, M., Shiraiwa, M., Koop, T., and Pöschl, U.: Kinetic  
372 regimes and limiting cases of gas uptake and heterogeneous reactions in atmospheric aerosols and  
373 clouds: a general classification scheme, *Atmos. Chem. Phys.*, 13, 6663-6686, 10.5194/acp-13-  
374 6663-2013, 2013.
- 375 Berkemeier, T., Steimer, S. S., Krieger, U. K., Peter, T., Pöschl, U., Ammann, M., and Shiraiwa,  
376 M.: Ozone uptake on glassy, semi-solid and liquid organic matter and the role of reactive oxygen  
377 intermediates in atmospheric aerosol chemistry, *Phys. Chem. Chem. Phys.*, 18, 12662-12674,  
378 10.1039/C6CP00634E, 2016.
- 379 Cappa, C. D., Zhang, X., Loza, C. L., Craven, J. S., Yee, L. D., and Seinfeld, J. H.: Application of  
380 the Statistical Oxidation Model (SOM) to secondary organic aerosol formation from  
381 photooxidation of C12 alkanes, *Atmos. Chem. Phys.*, 13, 1591-1606, 10.5194/acp-13-1591-2013,  
382 2013.
- 383 Chan, A. W. H., Kroll, J. H., Ng, N. L., and Seinfeld, J. H.: Kinetic modeling of secondary organic  
384 aerosol formation: effects of particle- and gas-phase reactions of semivolatile products, *Atmos.*  
385 *Chem. Phys.*, 7, 4135-4147, 10.5194/acp-7-4135-2007, 2007.
- 386 Finlayson-Pitts, B. J.: Reactions at surfaces in the atmosphere: integration of experiments and  
387 theory as necessary (but not necessarily sufficient) for predicting the physical chemistry of  
388 aerosols, *Phys. Chem. Chem. Phys.*, 11, 7760-7779, 10.1039/b906540g, 2009.
- 389 George, I. J., and Abbatt, J. P. D.: Heterogeneous oxidation of atmospheric aerosol particles by  
390 gas-phase radicals, *Nat. Chem.*, 2, 713-722, 10.1038/nchem.806, 2010.
- 391 Hanson, D. R., Ravishankara, A. R., and Solomon, S.: Heterogeneous reactions in sulfuric acid  
392 aerosols - A framework for model calculations, *Journal of Geophysical Research-Atmospheres*,  
393 99, 3615-3629, 10.1029/93jd02932, 1994.
- 394 Hearn, J. D., Lovett, A. J., and Smith, G. D.: Ozonolysis of oleic acid particles: evidence for a  
395 surface reaction and secondary reactions involving Criegee intermediates, *Phys. Chem. Chem.*  
396 *Phys.*, 7, 501-511, 10.1039/b414472d, 2005.
- 397 Herrmann, H., Ervens, B., Nowacki, P., Wolke, R., and Zellner, R.: A chemical aqueous phase  
398 radical mechanism for tropospheric chemistry, *Chemosphere*, 38, 1223-1232,  
399 [http://dx.doi.org/10.1016/S0045-6535\(98\)00520-7](http://dx.doi.org/10.1016/S0045-6535(98)00520-7), 1999.
- 400 Hosny, N. A., Fitzgerald, C., Vysniauskas, A., Athanasiadis, A., Berkemeier, T., Uygur, N.,  
401 Pöschl, U., Shiraiwa, M., Kalberer, M., Pope, F. D., and Kuimova, M. K.: Direct imaging of

402 changes in aerosol particle viscosity upon hydration and chemical aging, *Chem. Sci.*,  
403 10.1039/C5SC02959G, 2016.

404 Jenkin, M. E., Saunders, S. M., and Pilling, M. J.: The tropospheric degradation of volatile organic  
405 compounds: a protocol for mechanism development, *Atmos. Environ.*, 31, 81-104,  
406 [http://dx.doi.org/10.1016/S1352-2310\(96\)00105-7](http://dx.doi.org/10.1016/S1352-2310(96)00105-7), 1997.

407 Julin, J., Shiraiwa, M., Miles, R. E. H., Reid, J. P., Pöschl, U., and Riipinen, I.: Mass  
408 Accommodation of Water: Bridging the Gap Between Molecular Dynamics Simulations and  
409 Kinetic Condensation Models, *The Journal of Physical Chemistry A*, 117, 410-420,  
410 10.1021/jp310594e, 2013.

411 Kampf, C. J., Liu, F., Reinmuth-Selzle, K., Berkemeier, T., Meusel, H., Shiraiwa, M., and Pöschl,  
412 U.: Protein Cross-Linking and Oligomerization through Dityrosine Formation upon Exposure to  
413 Ozone, *Environ. Sci. Technol.*, 49, 10859-10866, 10.1021/acs.est.5b02902, 2015.

414 Kolb, C. E., Cox, R. A., Abbatt, J. P. D., Ammann, M., Davis, E. J., Donaldson, D. J., Garrett, B.  
415 C., George, C., Griffiths, P. T., Hanson, D. R., Kulmala, M., McFiggans, G., Pöschl, U., Riipinen,  
416 I., Rossi, M. J., Rudich, Y., Wagner, P. E., Winkler, P. M., Worsnop, D. R., and O' Dowd, C. D.:  
417 An overview of current issues in the uptake of atmospheric trace gases by aerosols and clouds,  
418 *Atmos. Chem. Phys.*, 10, 10561-10605, 10.5194/acp-10-10561-2010, 2010.

419 Lakey, P. S. J., Berkemeier, T., Tong, H., Arangio, A. M., Lucas, K., Pöschl, U., and Shiraiwa,  
420 M.: Chemical exposure-response relationship between air pollutants and reactive oxygen species  
421 in the human respiratory tract, *Sci. Rep.*, 6, 32916, 10.1038/srep32916, 2016a.

422 Lakey, P. S. J., Wisthaler, A., Berkemeier, T., Mikoviny, T., Pöschl, U., and Shiraiwa, M.:  
423 Chemical kinetics of multiphase reactions between ozone and human skin lipids: implications for  
424 indoor air quality and health effects, *Indoor Air*, Accepted Manuscript, 10.1111/ina.12360, 2016b.

425 Lowe, S., Partridge, D. G., Topping, D., and Stier, P.: Inverse modelling of Köhler theory – Part  
426 1: A response surface analysis of CCN spectra with respect to surface-active organic species,  
427 *Atmos. Chem. Phys.*, 16, 10941-10963, 10.5194/acp-16-10941-2016, 2016.

428 McNeill, V. F., Woo, J. L., Kim, D. D., Schwier, A. N., Wannell, N. J., Sumner, A. J., and Barakat,  
429 J. M.: Aqueous-phase secondary organic aerosol and organosulfate formation in atmospheric  
430 aerosols: A modeling study, *Environ. Sci. Technol.*, 46, 8075-8081, 10.1021/es3002986, 2012.

431 Partridge, D. G., Vrugt, J. A., Tunved, P., Ekman, A. M. L., Struthers, H., and Sorooshian, A.:  
432 Inverse modelling of cloud-aerosol interactions – Part 2: Sensitivity tests on liquid phase clouds  
433 using a Markov chain Monte Carlo based simulation approach, *Atmos. Chem. Phys.*, 12, 2823-  
434 2847, 10.5194/acp-12-2823-2012, 2012.

435 Pöschl, U., Rudich, Y., and Ammann, M.: Kinetic model framework for aerosol and cloud surface  
436 chemistry and gas-particle interactions - Part 1: General equations, parameters, and terminology,  
437 *Atmos. Chem. Phys.*, 7, 5989-6023, 2007.

438 Pöschl, U., and Shiraiwa, M.: Multiphase Chemistry at the Atmosphere–Biosphere Interface  
439 Influencing Climate and Public Health in the Anthropocene, *Chem. Rev.*, 115, 4440–4475,  
440 10.1021/cr500487s, 2015.

441 Riedel, T. P., Lin, Y. H., Zhang, Z., Chu, K., Thornton, J. A., Vizuete, W., Gold, A., and Surratt,  
442 J. D.: Constraining condensed-phase formation kinetics of secondary organic aerosol components  
443 from isoprene epoxydiols, *Atmos. Chem. Phys.*, 16, 1245-1254, 10.5194/acp-16-1245-2016, 2016.

444 Saunders, S. M., Jenkin, M. E., Derwent, R. G., and Pilling, M. J.: Protocol for the development  
445 of the Master Chemical Mechanism, MCM v3 (Part A): tropospheric degradation of non-aromatic  
446 volatile organic compounds, *Atmos. Chem. Phys.*, 3, 161-180, 10.5194/acp-3-161-2003, 2003.

447 Shiraiwa, M., Pfrang, C., and Pöschl, U.: Kinetic multi-layer model of aerosol surface and bulk  
448 chemistry (KM-SUB): the influence of interfacial transport and bulk diffusion on the oxidation of  
449 oleic acid by ozone, *Atmos. Chem. Phys.*, 10, 3673-3691, 2010.

450 Shiraiwa, M., Pfrang, C., Koop, T., and Pöschl, U.: Kinetic multi-layer model of gas-particle  
451 interactions in aerosols and clouds (KM-GAP): linking condensation, evaporation and chemical  
452 reactions of organics, oxidants and water, *Atmos. Chem. Phys.*, 12, 2777-2794, 10.5194/acp-12-  
453 2777-2012, 2012.

454 Shiraiwa, M., Yee, L. D., Schilling, K. A., Loza, C. L., Craven, J. S., Zuend, A., Ziemann, P. J.,  
455 and Seinfeld, J. H.: Size distribution dynamics reveal particle-phase chemistry in organic aerosol  
456 formation, *Proc. Natl. Acad. Sci. USA*, 110, 11746-11750, 10.1073/pnas.1307501110, 2013.

457 Shiraiwa, M., Berkemeier, T., Schilling-Fahnestock, K. A., Seinfeld, J. H., and Pöschl, U.:  
458 Molecular corridors and kinetic regimes in the multiphase chemical evolution of secondary organic  
459 aerosol, *Atmos. Chem. Phys.*, 14, 8323-8341, 10.5194/acp-14-8323-2014, 2014.

460 Smith, G. D., Woods, E., Baer, T., and Miller, R. E.: Aerosol uptake described by numerical  
461 solution of the diffusion - Reaction equations in the particle, *Journal of Physical Chemistry A*, 107,  
462 9582-9587, 10.1021/jp021843a, 2003.

463 Steimer, S. S., Berkemeier, T., Gilgen, A., Krieger, U. K., Peter, T., Shiraiwa, M., and Ammann,  
464 M.: Shikimic acid ozonolysis kinetics of the transition from liquid aqueous solution to highly  
465 viscous glass, *Phys. Chem. Chem. Phys.*, 17, 31101-31109, 10.1039/C5CP04544D, 2015.

466 Vieceli, J., Roeselova, M., Potter, N., Dang, L. X., Garrett, B. C., and Tobias, D. J.: Molecular  
467 dynamics simulations of atmospheric oxidants at the air-water interface: Solvation and  
468 accommodation of OH and O<sub>3</sub>, *Journal of Physical Chemistry B*, 109, 15876-15892,  
469 10.1021/jp051361+, 2005.

470 Worsnop, D. R., Morris, J. W., Shi, Q., Davidovits, P., and Kolb, C. E.: A chemical kinetic model  
471 for reactive transformations of aerosol particles, *Geophys. Res. Lett.*, 29, 57,  
472 10.1029/2002gl015542, 2002.

473 Zobrist, B., Soonsin, V., Luo, B. P., Krieger, U. K., Marcolli, C., Peter, T., and Koop, T.: Ultra-  
474 slow water diffusion in aqueous sucrose glasses, *Phys. Chem. Chem. Phys.*, 13, 3514-3526,  
475 10.1039/c0cp01273d, 2011.

476 Zuend, A., and Seinfeld, J. H.: A practical method for the calculation of liquid-liquid equilibria in  
477 multicomponent organic-water-electrolyte systems using physicochemical constraints, *Fluid  
478 Phase Equilibria*, 337, 201-213, 2013.